

Relaxation of ^{27}Al NMR in Aluminium Tribromide due to Raman Process

Noriaki Okubo^a, Mutsuo Igarashi^b, and Ryozi Yoshizaki^c

^a Institute of Physics, University of Tsukuba, Tsukuba 305, Japan

^b Department of Applied Physics, Gunma College of Technology, Maebashi 371, Japan

^c Institute of Applied Physics, University of Tsukuba, Tsukuba 305, Japan

Z. Naturforsch. **51a**, 277–282 (1996); received November 15, 1995

The nuclear spin-lattice relaxation of ^{27}Al NMR in AlBr_3 has been examined from 25 to 320 K. The result is analyzed using a theory of the Raman process based on covalency. A Debye temperature of 118 K is obtained together with a covalency larger than that obtained from the relaxation in the ^{81}Br NQR.

Key words: Aluminium tribromide; ^{27}Al NMR; Nuclear quadrupole relaxation; Raman process; Covalency.

Introduction

In the preceding paper [1] we dealt with the nuclear relaxation of bromine NQR in aluminium tribromide (AlBr_3) using a theory of the Raman process based on covalency [2]. Although the aluminium NQR is also reported in [3–6], there are some difficulties in applying the theory to the relaxation [1]. One of the difficulties originates from the large asymmetry parameter 0.747 [4]. This brings about considerable mixing among the states specified by the magnetic quantum number m . Then the transition probabilities for the quadrupolar relaxation involve large cross-terms of the matrix elements for transitions $\Delta m = \pm 1$ and $\Delta m = \pm 2$, and the existing theories cannot be applied. When the relaxation is treated in a strong external magnetic field, this problem is avoided since the Hamiltonian is then dominated by the Zeeman term; the eigen states can be specified properly by m . The purpose of the present paper is to show a way of handling the remaining difficulties and to provide information complementary to the bromine NQR study.

There is another motivation for the present study. AlBr_3 molecules are known to intercalate into graphite with Br_2 molecules to form ternary compounds [7]. We found that the ^{27}Al NMR of AlBr_3 changes drastically on intercalation [8]. However, there is little information about the relaxation in pure AlBr_3 . To ob-

tain the standard for comparison of the NMR is the second purpose.

1. Experimental

Since AlBr_3 is extremely hygroscopic, it is difficult to obtain ideal powder samples. The sample was prepared by melting and annealing as before, but a quartz ampoule was used in place of the pyrex one to avoid the ^{27}Al signal from pyrex glass.

The use of NMR for observing the ^{27}Al nuclei has an advantage over NQR: The resonance frequency is elevated up to a more reasonable value, and the observation is facilitated. The ^{27}Al NMR was observed with a pulse spectrometer (Matec Inc.). The relaxation was examined from 25 K to 320 K in a field of 7 T but also in 4.7 T at 77 K and room temperature. The spin echo signal after $\pi/2-\pi$ pulses was monitored. The spectrum was obtained as the envelope of the echo height measured with varying the frequency. The relaxation was examined by measuring the echo height at the center frequency, $S(t)$, at time t after saturation by another $\pi/2$ pulse. T_2 was 2.5 ± 0.5 ms and T_2^* was 16 ± 4 μs , typically at 77 K.

2. Results and Discussion

2.1 Origin of Relaxation

Figure 1 shows the line shape of ^{27}Al NMR. The pattern was almost independent of the temperature,

Reprint requests to Dr. N. Okubo.

0932-0784 / 96 / 0400-0277 \$ 06.00 © – Verlag der Zeitschrift für Naturforschung, D-72072 Tübingen



Dieses Werk wurde im Jahr 2013 vom Verlag Zeitschrift für Naturforschung in Zusammenarbeit mit der Max-Planck-Gesellschaft zur Förderung der Wissenschaften e.V. digitalisiert und unter folgender Lizenz veröffentlicht: Creative Commons Namensnennung-Keine Bearbeitung 3.0 Deutschland Lizenz.

Zum 01.01.2015 ist eine Anpassung der Lizenzbedingungen (Entfall der Creative Commons Lizenzbedingung „Keine Bearbeitung“) beabsichtigt, um eine Nachnutzung auch im Rahmen zukünftiger wissenschaftlicher Nutzungsformen zu ermöglichen.

This work has been digitalized and published in 2013 by Verlag Zeitschrift für Naturforschung in cooperation with the Max Planck Society for the Advancement of Science under a Creative Commons Attribution-NoDerivs 3.0 Germany License.

On 01.01.2015 it is planned to change the License Conditions (the removal of the Creative Commons License condition “no derivative works”). This is to allow reuse in the area of future scientific usage.

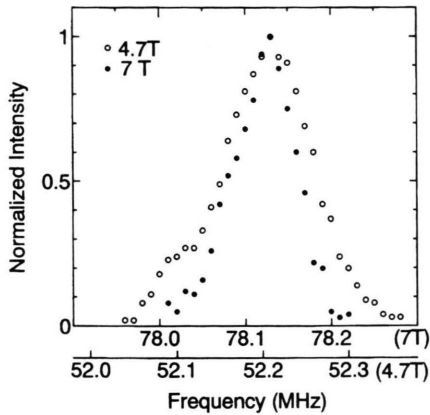


Fig. 1. The line shape of ^{27}Al NMR in AlBr_3 at room temperature. The pattern for 7 T is so shifted that the peak is superposed on that for 4.7 T.

but somewhat dependent on the setting of the sample in the magnet because it was polycrystalline. However, it roughly corresponds to the powder pattern [9] derived with the coupling constant $e^2 Q q = 13.57$ MHz and the asymmetry parameter $\eta = 0.747$ [4], and the width is nearly inversely proportional to the strength of the field. Therefore the observed signal is the central transition ($m = 1/2$ to $-1/2$) broadened mainly by the second-order perturbation of the quadrupolar interaction.

The magnetic relaxation of the system with spin $I = 5/2$ is governed by three characteristic times, under an initial condition symmetrical about $\pm m$. They are written as $(2W)^{-1}$, $(12W)^{-1}$, and $(30W)^{-1}$, when the transition probability from the level m to $m+1$, $P(m, m+1)$, is written as $W(I+1)(I-m+1)$ [10]. On the other hand, the quadrupolar relaxation is governed by three characteristic times, which are the inverse of the roots of the following secular equation [10]:

$$100\lambda^3 + 280\lambda^2(W_1 + W_2) + 3\lambda(40W_1^2 + 208W_1W_2 + 45W_2^2) + 36W_1W_2(4W_1 + 7W_2) = 0, \quad (1)$$

where W_1 and W_2 are defined with $P(m, m+\mu)$ ($\mu = 1, 2$) as

$$P(m, m+1) = \frac{(2m+1)^2(I-m)(I+m+1)}{2I(2I-1)^2} W_1, \quad (2)$$

$$P(m, m+2) = \frac{(I-m-1)(I+m+2)(I-m)(I+m+1)}{2I(2I-1)^2} W_2.$$

The magnetization recovery curve can be derived by regarding the effect of application of saturating $\pi/2$ pulse as only equalizing the populations of two levels corresponding to the frequency. For the magnetic relaxation of the system it can be shown that

$$[S(\infty) - S(t)]/S(\infty) = \frac{1}{35} \exp(-2Wt) + \frac{8}{45} \exp(-12Wt) + \frac{50}{63} \exp(-30Wt). \quad (3)$$

On the other hand, for the quadrupolar relaxation the pre-exponential coefficients depend on the ratio of W_1 and W_2 but, as shown later, we are particularly concerned with the case $W_1 = W_2 (\equiv W)$. Then

$$[S(\infty) - S(t)]/S(\infty) = \frac{1}{35} \exp\left(-\frac{4}{5}Wt\right) + \frac{50}{63} \exp\left(-\frac{3}{2}Wt\right) + \frac{8}{45} \exp\left(-\frac{33}{10}Wt\right). \quad (4)$$

When the observed recovery curves are fitted by both equations, a clear difference appears only at values of $[S(\infty) - S(t)]/S(\infty)$ smaller than 10^{-1} . An example is shown in Figure 2. The signal-to-noise ratio was not sufficient to discriminate the two relaxation mechanisms by this method. However, when the recovery curves for all temperatures are fitted by (4), W shows T^2 dependence at high temperatures, as shown in Figure 3. This suggests that the relaxation is governed by the Raman process.

In the region including 77 K, W increased as the temperature increased, and the relaxation was almost independent of the strength of magnetic field at 77 K.

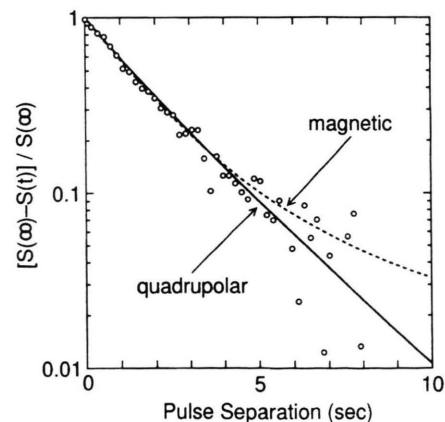


Fig. 2. An example of the magnetization recovery curve at 210 K in the field of 7 T.

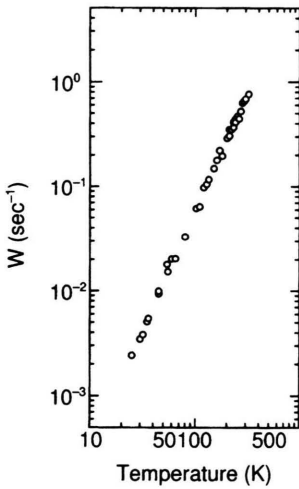


Fig. 3. Temperature dependence of the transition probability W of the ^{27}Al -NMR line in AlBr_3 .

If the BPP type relaxation mechanism was dominant, the relaxation rate should be inversely proportional to the square of the strength of the magnetic field in the region where it increases with increasing temperature, whether the relaxation is magnetic or quadrupolar. Therefore, the BPP type mechanism is excluded.

2.2 Expression for Raman Process

In the following the Raman process is assumed. For brevity, in the dimer Al_2Br_6 [11], three mirror planes perpendicular to each other are assumed; the bisecting plane of the terminal bonds contains the bridging bonds, and vice versa. The bridging Br atoms are numbered as 1 and 2, and the terminal ones as 3 and 4, in accordance to [12]. Furthermore, in order to apply Yosida and Moriya's theory assuming the equivalence of the ions [2], the four Br ions are assumed to be equivalent, so that we do not expect complete numerical agreement between the theory and the experiment. Then $P(m, m + \mu)$ ($\mu = 1, 2$) due to the Raman process is given for any spin I by

$$P(m, m + \mu) = \frac{A'^2 c^3 |Q_{\mu m}|^2}{2\pi^3 a^7 d^2 v_s^3} \cdot T^{*2} \sum_{\phi} \sum_{v=1}^3 N_{\mu v}(\phi) D_v(T^*, \phi), \quad (5)$$

$$A' = \frac{3e^2 Q \langle r^{-3} \rangle}{10I(2I-1)}, \quad Q_{\mu m} = \langle m + \mu | Q_{\mu} | m \rangle,$$

$$Q_{\pm 1} = \frac{1}{2}(I_{\pm} I_z + I_z I_{\pm}), \quad Q_{\pm 2} = I_{\pm}^2.$$

The notation is the same as in [1]. In the present case, $\langle \rangle$ means the expectation value with respect to the valence p electron of Al atom. The sound velocity v_s is related to the Debye temperature θ_D by

$$\hbar \omega_D = \hbar v_s k_D = k_B \theta_D. \quad (6)$$

Summation over the angle made by any bond pair, ϕ , has been introduced to avoid the use of large v in applying the theory to the case involving several different bond angles, and instead $N_{\mu v}$ and D_v ($v = 1$ to 3) have been left to be functions of ϕ .

Since the sample was, though not powder, polycrystalline, $N_{\mu v}$ must be averaged about the orientation of the field H_0 . After averaging, $N_{\mu v}$ is expressed with a measure of covalency, λ , and its first and second derivatives with respect to r , λ' and λ'' , as follows:

$$N_{11} = N_{12} = N_{13} = 8 \left[\frac{1}{15} (77 \cos^2 \phi + 1) u^2 + \frac{1}{15} (3 \cos^2 \phi - 1) v^2 + \lambda^2 + \frac{2}{15} (11 \cos^2 \phi - 1) uv + \frac{8}{3} \lambda u + \frac{4}{15} \lambda v \right],$$

$$N_{21} = N_{22} = N_{23} = N_{11}/4, \quad (7)$$

where

$$u = \frac{1}{2} a \lambda' - \lambda, \quad v = 4\lambda - \frac{5}{2} a \lambda' + \frac{1}{2} a^2 \lambda''.$$

Equation (7) can be applied to any equivalent bond pair in NMR of powders. The derivation of these expressions is given in the Appendix.

$D_v(T^*)$ is defined as

$$D_v(T^*) = T^* \int_0^{1/T^*} \frac{x^2 e^x}{(e^x - 1)^2} L_v(c T^* x) dx, \quad (8)$$

where $x = \hbar \omega / k_B T$, ω being the angular frequency of the phonons. $L_v(c T^* x) = L_v(ka)$ has generally the following forms:

$$L_1(ka) = \{S_1 S_2\}_k^2 = \left[-\frac{1}{2} f(\sqrt{2(1 + \cos \phi)} ka) + \frac{1}{2} f(\sqrt{2(1 - \cos \phi)} ka) \right]^2,$$

$$L_2(ka) = \{C_1 C_2\}_k^2 = [1 - 2 f(ka) + \frac{1}{2} f(\sqrt{2(1 + \cos \phi)} ka) + \frac{1}{2} f(\sqrt{2(1 - \cos \phi)} ka)]^2,$$

$$L_3(ka) = 2 \{S_1 S_2 C_1 C_2\}_k = 2 \left[-\frac{1}{2} f(\sqrt{2(1 + \cos \phi)} ka) + \frac{1}{2} f(\sqrt{2(1 - \cos \phi)} ka) \right] \cdot [1 - 2 f(ka) + \frac{1}{2} f(\sqrt{2(1 + \cos \phi)} ka) + \frac{1}{2} f(\sqrt{2(1 - \cos \phi)} ka)],$$

where

$$S_n = \sin(ak \cdot n), \quad C_n = \cos(ak \cdot n) - 1, \\ f(y) = \frac{\sin y}{y} \quad (9)$$

and $\{ \}_k$ means the average about the direction of k , k being the wave vector of the phonon, and k its magnitude. n denotes the unit vector along the bond.

Since W_μ ($\mu = 1, 2$) is related with $P(m, m + \mu)$ by (2) and $N_{2v} = N_{1v}/4$ by (7), we obtain $W_1 = W_2 = W$. This equality holds for any value of spin. W for $I = 5/2$ is then written as

$$W = \frac{9e^4 Q^2 \langle r^{-3} \rangle^2 c^3}{1000 \pi^3 a^7 d^2 v_s^3} T^{*2} \sum_{\phi} \sum_{v=1}^3 N_{1v}(\phi) D_v(T^*, \phi). \quad (10)$$

2.3 Estimation of Debye Temperature

Introducing a scaling time τ defined as

$$\tau^{-1} = \frac{9e^4 Q^2 \langle r^{-3} \rangle_{\text{Al}}^2 c^3}{1000 \pi^3 a^7 d^2 v_s^3} N_{11}(0), \quad (11)$$

(10) can be reduced to a form convenient for fitting:

When bridging bonds are neglected,

$$WT^{-2} = (\tau \theta_D^2)^{-1} \left[\sum_{v=1}^3 D_v(T^*, 0) + \varepsilon(\phi_{34}) \sum_{v=1}^3 D_v(T^*, \phi_{34}) \right], \quad (12)$$

and when bridging bonds are also taken into account,

$$WT^{-2} = (\tau \theta_D^2)^{-1} \left[2 \sum_{v=1}^3 D_v(T^*, 0) + \varepsilon(\phi_{12}) \sum_{v=1}^3 D_v(T^*, \phi_{12}) + \varepsilon(\phi_{34}) \sum_{v=1}^3 D_v(T^*, \phi_{34}) + 4\varepsilon(\phi_{13}) \sum_{v=1}^3 D_v(T^*, \phi_{13}) \right]. \quad (13)$$

In (12) and (13), $\phi_{n,n'}$ denotes the angle between the bonds n and n' , and

$$\varepsilon(\phi_{n,n'}) = \frac{N_{11}(\phi_{n,n'})}{N_{11}(0)}.$$

By fitting (12) or (13) to the experimental result, we can determine θ_D together with τ as fitting parameters. The relation

$$\lambda \propto \exp(-r/\varrho) \quad (14)$$

Table 1. Values of N_{1v} ($v = 1$ to 3) for the bond pair making the angle ϕ , in unit of λ^2 . The value of ϕ_{13} was calculated from the values of ϕ_{12} and ϕ_{34} [11], assuming three mirror planes in Al_2Br_6 dimer.

ϕ	ϕ_{nn} ($= 0^\circ$)	ϕ_{12} ($= 97.9^\circ$)	ϕ_{34} ($= 114.7^\circ$)	ϕ_{13} ($= 110.8^\circ$)
$N_{1v}(\phi)$	746.4	167.8	-109.4	-37.9

Table 2. Debye temperature θ_D , scaling time τ , and a measure of covalency λ .

	θ_D (K)	τ (s)	λ
Bridging neglected	117.8	7.41	0.150
Bridging included	117.6	15.15	0.104

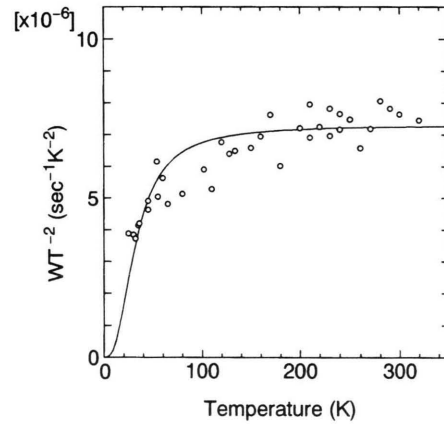


Fig. 4. The result of a least-squares-fitting of (12). The result for (13) is omitted because it is almost superposed by that for (12).

was assumed with a value of 0.345 \AA for the repulsive range parameter ϱ as before [1, 2]. Using $a = 2.28 \text{ \AA}$ as an average for terminal bonds we have $u = -4.304 \lambda$ and $v = 42.359 \lambda$. The values of N_{1v} calculated from (7) are given in Table 1. A value of 2.753 was used for $c = k_D a$. The integration in (8) was carried out numerically. Table 2 and Fig. 4 show the results of a least-square-fitting. The present value of θ_D for Al atoms, 117.8 or 117.6 K, is much higher than that obtained for Br atoms, 67.6 K [1]. For AlBr_3 the value of θ_D has not been determined either from the experiment of the specific heat or from the temperature factor in the X-ray analysis. In the case of SbCl_3 [13] a value of θ_D higher than that for the halogen atoms was calculated for the central metal from the temperature factor. For

v_s we obtain a value of 1.30 or 1.29×10^5 cm/sec by means of [6].

2.4 Estimation of Covalency

Now we can estimate λ from τ using (11). The $e^2 Q \langle r^{-3} \rangle$ is given by $(5/4) e^2 Q q_{\text{at}}$, $e^2 Q q_{\text{at}}$ being the quadrupole coupling constant for the free atom, reported to be 37.52 MHz for ^{27}Al [14]. We obtained the values of λ in Table 2. λ corresponds to the number of electrons on each bond, effective for the largest component of the EFG along the bond [1, 13]. Therefore, when there are several bonds, λ should be compared not with the ratio $f = e^2 Q q_{\text{mol}} / e^2 Q q_{\text{at}}$ for the whole molecule but with f for each bond.

Casabella *et al.* [4] analyzed the ^{27}Al NQR frequency with the expression

$$\frac{e^2 Q q_{\text{mol}}}{e^2 Q q_{\text{at}}} = \frac{(A_M - B_M)}{2} [1 + \cot^2(\phi_{12}/2)] (1 + \varrho_M \epsilon), \quad (15)$$

where A_M denotes the electron population of each terminal orbital of the Al atom and B_M that of the bridging one. From the Br NQR frequency they determined the excess of electrons on Br atoms and then estimated the net electron loss ϱ_M of Al atom as 1.74. Using a value of 0.25 for ϵ , they obtained values of 0.46 for A_M and 0.17 for B_M . Since (15) is a sum of the contributions from two terminal and two bridging bonds to the EFG component along the direction connecting two bridging Br atoms, the contribution of one terminal bond to the EFG along the bond is given by

$$(A_M/2) [1 + \cot^2(\phi_{12}/2)] (1 + \varrho_M \epsilon) / [3 \sin^2(\phi_{34}/2) - 1],$$

which is evaluated to be 0.51. Similarly, the contribution of one bridging bond is given by

$$(B_M/2) [1 + \cot^2(\phi_{12}/2)] (1 + \varrho_M \epsilon),$$

and this is evaluated to be 0.21.

The values of λ in Table 2 should be compared with the average of these values. In the preceding paper [1] the low value of λ for Br atoms was attributed to the low estimate of θ_D . For Al atom, certainly, corresponding to the much higher θ_D , a much larger λ has been obtained. However, the values of λ are still smaller than either value of f for each bond. Since in (12) and (13) the first terms are positive and dominant, we may expect that these equations approximately give the lower and upper limits of the observed transi-

tion probability W_{obs} , respectively. However, the present situation is expressed in terms of W as

$$\begin{aligned} W_{\text{obs}} &< W_{\text{calc}} (\text{bridging neglected}) \\ &< W_{\text{calc}} (\text{bridging included}), \end{aligned}$$

whichever value of f for each bond is used for λ .

2.5 Concluding Remarks

By the use of NMR the problem originating from the mixing of spin states in the NQR has been avoided. An approach to the quadrupolar relaxation in a multi-bond system by means of the theory of the Raman process has been shown. The estimated covalency is relatively small compared with the values estimated from the NQR frequencies. Nevertheless, taking into account the crudeness involved in the theory and the present analysis, it should still be noted that the theory of the Raman process gives a substantially correct order of magnitude of covalency.

Appendix

Derivation of $N_{\mu\nu}$

In (4.35) and (4.36) of [2],

$$N_{\mu\nu} = \sum_{n, n'} \sum_{pp'} W_{\mu n}^* (\sigma\sigma') W_{\mu n'} (\sigma\sigma')$$

is expressed with the direction cosines of bonds \mathbf{n} and \mathbf{n}' in the coordinate system whose z axis is taken along the external magnetic field \mathbf{H}_0 . Due to the nature of the direction cosines, $N_{\mu\nu}$ can be written as a sum of terms consisting of the powers only of the direction cosines to the z axis, γ_n and $\gamma_{n'}$. To average the powers

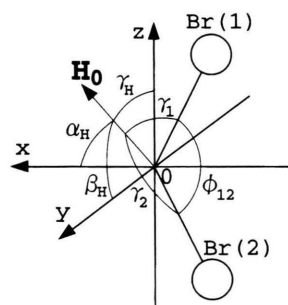


Fig. 5. The coordinate system for the calculation of the average of $N_{\mu\nu}$ with respect to the direction of the field \mathbf{H}_0 . The Al atom is taken as the origin. The symbols γ_1 , γ_2 , α_H , β_H , and γ_H denote the direction cosines, while ϕ_{12} denotes the angle.

of, say γ_1 and γ_2 with respect to the direction of \mathbf{H}_0 , we introduce the new coordinate system shown in Fig. 5, where the $-x$ axis is taken as the bisector of the bond angle $\text{Br}(1)\text{--Al--Br}(2)$, and the z axis is taken in the plane of these bonds. Then γ_1 is written as the inner product of the unit vector along the bond $\text{Al--Br}(1)$, $(-\cos(\phi_{12}/2), 0, \sin(\phi_{12}/2))$, and the unit vector along the field, $(\alpha_H, \beta_H, \gamma_H)$, as

$$\gamma_1 = -\alpha_H \cos(\phi_{12}/2) + \gamma_H \sin(\phi_{12}/2).$$

Similarly,

$$\gamma_2 = -\alpha_H \cos(\phi_{12}/2) - \gamma_H \sin(\phi_{12}/2).$$

Then we get

$$\begin{aligned}\overline{\gamma_1^2} &= \overline{\gamma_2^2} = 1/3, \\ \overline{\gamma_1^4} &= \overline{\gamma_2^4} = 1/5,\end{aligned}$$

$$\begin{aligned}\overline{\gamma_1 \gamma_2} &= (1/3) \cos \phi_{12}, \\ \overline{\gamma_1^2 \gamma_2^2} &= (1/15)(2 \cos^2 \phi_{12} + 1), \\ \overline{\gamma_1^3 \gamma_2} &= \overline{\gamma_1 \gamma_2^3} = (1/5) \cos \phi_{12}.\end{aligned}$$

Here the averages

$$\overline{\alpha_H^2} = \overline{\gamma_H^2} = 1/3, \quad \overline{\alpha_H^4} = \overline{\gamma_H^4} = 1/5, \quad \overline{\alpha_H^2 \gamma_H^2} = 1/15,$$

and

$$\overline{\alpha_H^3 \gamma_H} = \overline{\alpha_H \gamma_H^3} = 0$$

have been used. Since the coordinate axes have been chosen irrespectively of the principal axis system, the above result can be generalized to any bond pair. Substitution of the results into the direction averages in $\Sigma_{pp'} W_{\mu n}^*(\sigma\sigma') W_{\mu n'}(\sigma\sigma')$ yields the expressions for $N_{\mu\nu}$ in the text.

- [1] N. Okubo, M. Igarashi, R. Yoshizaki, Z. Naturforsch. **50a**, 737 (1995).
- [2] K. Yosida and T. Moriya, J. Phys. Soc. Japan **11**, 33 (1956).
- [3] R. G. Barnes and S. L. Segel, J. Chem. Phys. **25**, 180 (1956).
- [4] P. A. Casabella, P. J. Bray, and R. G. Barnes, J. Chem. Phys. **30**, 1393 (1950).
- [5] T. Okuda, H. Terao, O. Ege, and H. Negita, J. Chem. Phys. **52**, 5489 (1970).
- [6] N. Weiden and A. Weiss, J. Magn. Reson. **20**, 334 (1975).
- [7] H. Zabel and S. A. Solin eds., Graphite Intercalation Compounds I, Springer, Berlin 1990.
- [8] To be published elsewhere.
- [9] G. H. Stauss, J. Chem. Phys. **40**, 1988 (1964).
- [10] E. R. Andrew and D. P. Tunstall, Proc. Phys. Soc. **78**, 1 (1961).
- [11] P. A. Renes and C. H. Mac Gillavry, Rec. Trav. Chim. **64**, 275 (1945).
- [12] E. A. C. Lucken, Nuclear Quadrupole Coupling Constants, Academic Press, New York 1969.
- [13] N. Okubo and Y. Abe, Z. Naturforsch. **49a**, 680 (1994).
- [14] T. P. Das and E. L. Hahn, Nuclear Quadrupole Resonance Spectroscopy, Solid State Physics, F. Seitz and D. Turnbull, Academic Press, New York 1958, Supplement (1994).